ISSN 2347-3487

Image Comparisons Among Analysis, Simulation and Experimental Solutions About Stress Distribution in Rings Loaded by Multiple Symmetrical Radial Forces

Wang Peng, Xie Lili, Yica Sun, Yongshu Jiao, Pang Dongqing
Hebei University of Technology, Xiping road 5342#,Tianjin, P.R. China
wangpeng1027@126.com
Tianjin Vocational College, Tianjin beichen district luohe road no. 2
shelly0313@126.com
Hebei University of Technology. Xiping road 5342#,Tianjin, P.R. China
sychebut@126.com
Hebei University of Technology, Xiping road 5342#,Tianjin, P.R. China
yongshujiao@126.com
Tianjin University, Weijin road 172#,Tianjin, P.R. China
pangdongqing@tju.edu.cn

ABSTRACT

The theorem of energy valley state and a particular solution of Airy biharmonic equation will be used in the stress analysis in the rings loaded by the multiple- fold symmetrical forces to obtain stresses formulas. The varied stress graphs have been plotted with these formulas and FEM, revealing their periods of symmetry of forces.

Key words

Rings loaded by the multiple- fold symmetrical force; Stress analysis; FEM solutions

Academic Discipline

Scientific study

SUBJECT CLASSIFICATION

Stress calculation

METHOD

Survey

Council for Innovative Research

Peer Review Research Publishing System

Journal: JOURNAL OF ADVANCES IN PHYSICS

Vol. 6, No. 3

japeditor@gmail.com, www.cirjap.com

ISSN 2347-3487

1. INTRODUCTION

Regarding the stress calculation problem in rings loaded by the double symmetrical radial force receives arguments for hundred years [1-19], less much refers to the problem on the stress estimation in rings loaded by multiple symmetrical radial forces , therefor nobody concerns with it.

The authors thought, this is a difficulty to face us because people lack two keys. The author has given these two keys: 1.the valley theorem.2. Solutions satisfy the Airy equation only suitable for the stress distribution in rings, but they are high energy solutions. Only after combining these two keys to each other, not only we can solve the stress computation about the double fold, but also the multiple fold symmetrical forces in rings. However, the authors have given the fundamental formulas merely, have not given the corresponding images, also have not given image comparisons among analysis, simulation and experimental solutions. This is the goal of this article, making up its insufficiency, to benefit the application for formulas.

2. THE STRESS SITUATION SUPPOSITION

2.1 Situations used for the analysis solutions

As like Fig. 1-a shows that the ring has double-fold symmetrical radial forces. In order to for more comprehensive, we attempts also to propose triply and four- fold symmetrical radial forces, like Fig. 1-b, c show, in favor of the application of stress distribution in rings. These radial forces are distribution ones, used for the analysis solutions.

2.2 Situations used for finite element solutions

Fig. 2 shows respectively that double-fold symmetrical radial forces, triply and four- fold symmetrical radial forces, acting on the outer boundaries, used for FEM calculation.

3. FORMULAS USED FOR ANALYSIS SOLUTIONS

3.1 Double fold symmetry of loads[19]

$$\sigma_{\theta\theta}(\alpha,\theta) = -\frac{1}{2}\frac{F}{Br_0}[g(\alpha)(cos\theta - \frac{2}{\pi}) + (B/1-\alpha_0)\cdot\frac{2}{\pi}] \quad \text{(circumferential stress)}$$

$$\sigma_{rr}(\alpha,\theta) = -\frac{1}{2}\frac{F}{Br_o}[h(\alpha)(cos\theta - \frac{2}{\pi})] \quad \text{(radial normal stress)}$$

$$\sigma_{r\theta}(\alpha,\theta) = -\frac{1}{2}\frac{F}{Br_o}h(\alpha)\sin\theta \quad \text{(shear stress)}$$

$$\tau_{\max}(\alpha,\theta) = \frac{1}{2}\sqrt{[\sigma_{\theta\theta}(\alpha,\theta) - \sigma_{rr}(\alpha,\theta)]^2 + 4\sigma_{r\theta}^2(\alpha,\theta)} \quad \text{(equi-maximal shear stress)}$$

where

$$g(\alpha) = [-1/\alpha + \xi(3\alpha - \alpha_i^2/\alpha^3]$$

$$h(\alpha) = [-1/\alpha + \xi(\alpha + \alpha_i^2/\alpha^3)]$$

$$B = \int_{\alpha_i}^{1} g(\alpha)d\alpha = \int_{\alpha_i}^{1} h(\alpha)d\alpha = ln\alpha_i + \xi(1-\alpha_i^2)$$

ISSN 2347-3487

$\xi = r_o^2/(r_o^2 + r_i^2) = 1/(1+\alpha_i^2)$, $\alpha = r/r_o$,

$\alpha_i = r_i/r_o$ is the ratio of inner and outer radios

3.2 Triply fold- symmetry of loads

$$\sigma_{\theta\theta}(\alpha,\theta) = -\frac{1}{2}\frac{F}{Br_0}[g(\alpha)(cos\theta - 1 + 0.173) + (^{(1-0.173)B}/_{1-\alpha_0})] \quad \text{(circumferential stress)}$$

$$\sigma_{rr}(\alpha,\theta) = -\frac{1}{2}\frac{F}{Br_0}[h(\alpha)(cos\theta - 1 + 0.173)] \quad \text{(radial normal stress)} \quad \sigma_{r\theta}(\alpha,\theta) = -\frac{1}{2}\frac{F}{Br_o}h(\alpha)\sin\theta$$

(shear stress , its sign in 1/4 ring is not changed).

$$\tau_{\max}(\alpha,\theta) = \frac{1}{2}\sqrt{[\sigma_{\theta\theta}(\alpha,\theta) - \sigma_{rr}(\alpha,\theta)]^2 + 4\sigma_{r\theta}^2(\alpha,\theta)} \quad \text{(equi-maximal shear stress)}$$

These stresses satisfy the balance of forces and the moment. They are only suitable for the scope from $\theta = -60^\circ$ to $\theta = 60^\circ$. When θ surpasses this scope, they should be symmetrically rotated relatively to $\theta = 0^\circ$ or $\theta = 60^\circ$. Figure 3 to 10 show respectively circumferential, radial normal stresses, shear stress and the equi-maximal shear stress for the thin and thick rings with $\alpha_i = 0.7$ and $\alpha_i = 0.5$, loaded by triply fold- symmetry of the forces. These figures all are obtained by rotating the first period until 6 periods are completed.

3.3 Four- fold- symmetry of loads

$$\sigma_{\theta\theta}(\alpha,\theta) = -\frac{\sqrt{2}}{2}\frac{F}{Br_0}[g(\alpha)(cos\theta - 1 + 0.19) + (^{B}/_{1-\alpha_i})\cdot(1-0.19)]..... \quad \text{(circumferential stress)}$$

$$\sigma_{rr}(\alpha,\theta) = -\frac{\sqrt{2}}{2}\frac{F}{Br_0}h(\alpha)(cos\theta - 1 + 0.19) \quad \text{(radial normal stress)}$$

$$\sigma_{\theta r}(\alpha,\theta) = -\frac{\sqrt{2}}{2}\frac{F}{Br_0}[h(\alpha)\sin\theta]..... \quad \text{(shear stress)}$$

where the rang of θ is from 0° to $\pi/4$, i.e. the first period. Equi-maximal shear stress is

$$\tau_{\max}(\alpha,\theta) = 1/2\sqrt{[\sigma_{\theta\theta}(\alpha,\theta) - \sigma_{rr}(\alpha,\theta)]^2 + 4\sigma_{r\theta}^2(\alpha,\theta)} \qquad \pi/4 \geq \theta \geq -\pi/4$$

The signs of shear stress are not changed in 1/4 ring. There are also the following expressions for above all formulas

$$g(\alpha) = [-1/\alpha + \xi(3\alpha - \alpha_i^2/\alpha^3]$$

$$h(\alpha) = [-1/\alpha + \xi(\alpha + \alpha_i^2/\alpha^3)]$$

$$B = \int_{\alpha_i}^{1} g(\alpha)d\alpha = \int_{\alpha_i}^{1} h(\alpha)d\alpha = ln\alpha_i + \xi(1-\alpha_i^2)$$

$\xi = r_o^2/(r_o^2 + r_i^2) = 1/(1+\alpha_i^2)$, $\alpha = r/r_o$, $\alpha_i = r_i/r_o$

In above , all various sort of stresses satisfy the moment balance and the microscopic and macroscopic balance of forces. Stress calculations inside the ring have been completed and their stripe distribution maps for the equi-maximal shear stress $\tau_{\max}$ have been plotted to show in section 4.

ISSN 2347-3487

4. FINAL IMAGES

4.1 Double fold symmetry of loads

It is note that only the equi-maximal shear stress are shown for analysis solution and FEM simulation images for double fold symmetry of loads in Fig.3 and Fig.4.

4.2 Triply fold- symmetry of loads

In the following various figures(Fig.5-Fig.14), the right is the FEM simulation result; the left is analysis solution images in favors to comparison. Fig.5-Fig.12 show images for triply fold- symmetry of loads.

4.3 Four fold- symmetry of loads

Fig.13-Fig.14 show images for four fold- symmetry of loads.

5. PHOTO ELASTICITY TESTING RESULTS

It is note that all of the following photos are selected from Frocht 'work. [5]

5.1 The graphs for the rings

The equi-maximum shear stress for the double fold- symmetrical forces on rings are shown in Fig.15.

5.2 The graphs for solid discs and 8 hole ring

This article discusses the stress distribution in the loaded ring. However, in order to observe to the practical situations, Fig.16 shows photo elasticity testing results [5]in solid discs and 8 hole ring.

6. DISCUSSRS

6.1 The stress analysis, simulation and experimental solution images in rings are basically consistent to each other, all display the corresponding symmetry.

6.2 Analysis and experimental solution images are more consistent, because in photo elasticity experiments, clamp plats are pressed on the outer surface of the ring to avoid the function of the point force. Therefore, analysis solution supposition is consistent with the experimental supposition .However, the FEM solutions pay attention to a point force acting on the outside surface of the ring and its elastic behavior only to give the influence upon its close neighbor near the outer surface of the ring. This point force action has not penetrated into inside of the ring, including its influence on the inner surface of the ring. This shows that point force function only limits nearby the outer wall, it does not to have the influence on the other parts between two symmetrical radial forces. Therefore, the analysis, simulation, and experimental solution images for the circumferential, radial, shear stress distribution images are all consistent to each other in these parts between two symmetrical radial forces.

6.3 Because of the above reason, the FEM solution images for shear stress distribution reveal a performance more prominent in the ring outside surface, moreover colors both sides of a point force are distinct difference. One is red, other is blue. (please note that both red and blue colors all represent large absolute amplitude for shear stress respectively, but only then the slight tint represents a little amplitude).The reason possibly is that people observe the section plane in two opposite directions, respectively perpendicular (i.e. facing) to it. Because the shear stress direction in both sides of a point force is same, relying on the right hand law, the signs of shear stresses on both sides of the point force are respectively plus and minus symbols with opposite signs. However, regarding equi-maximum shear stress images, there is no any question about opposite signs because the formula for analysis solution of equi-maximum shear stress is :

ISSN 2347-3487

$$\tau_{\max}(\alpha,\theta) = 1/2\sqrt{[\sigma_{\theta\theta}(\alpha,\theta) - \sigma_{rr}(\alpha,\theta)]^2 + 4\sigma_{r\theta}^2(\alpha,\theta)}$$

But Von_Mises_ Stress is used as the formula for FEM solution：

$$\bar{\sigma} = \frac{1}{\sqrt{2}}\left[(\sigma_{xx} - \sigma_{yy})^2 + (\sigma_{xx} - \sigma_{zz})^2 + (\sigma_{yy} - \sigma_{zz})^2 + 6(\sigma_{xy}^2 + \sigma_{yz}^2 + \sigma_{zx}^2)\right]^{1/2}$$

where σ_{xx}、σ_{yy} and σ_{zz} are respectively normal stresses and shear stress along x、y and z axis .Both ones are basically consistent with each other for the plane stress field, because it is the square for shear stress in these two expressions. Thus,.the graphs of the equi-maximum shear stress for analysis solutions are consistent with simulation images by using Von_Mises_Stress formula, particularly in the inside of the ring between two radial forces.

6.4. There are different assumptions in the begging about force distribution. The forces are uniform distribution inside of the ring used for the analysis solutions, So the radial normal stresses and shear stresses are zero at the outer wall, which is the boundary conditions but they are not zero in the middle of the ring with a red color.. However, the forces are concentrated point forces at the outer wall used for FEM solutions. Thus, the analysis solutions are not the same as the FEM solutions for radial normal stress and shear stress. These stresses are all not zero for latter one near the concentrated force acting points.

6.5 There is no boundary condition for the circumferential stress and it is much higher than radial normal stress and shear stress. Especially for the thin ring, the circumferential stress near inner and outer boundaries is very large, but opposite in sign. So the analysis, simulation, experiment image are consistent with each other. However, with the increase of thickness, the absolute value (i.e. tensile and compressive stress)of the circumferential stress at the outer boundary is greatly reduced, but effect of the radial stress and shear stress increase. Therefore, the color around the centric part of the ring reveals red along the symmetrical force direction. And the maximum shear stress distribution in the image also has the same performance (It is more obvious as shown in Figure 12). At this time, so far as two or three, four fold symmetry of radial forces, analysis, simulation, experiment images are all consistent with each other around this centric part.

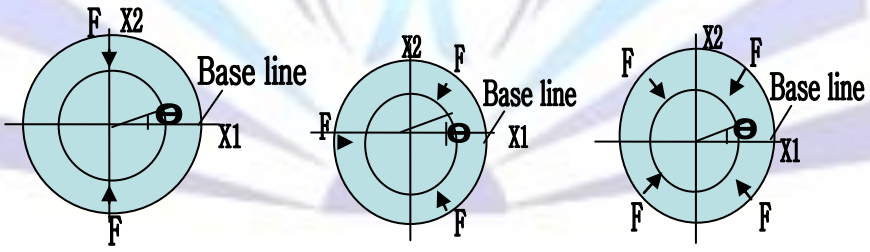

(a) (b) (c)

Figure 1 Symmetrical distributed forces F acting inside of the ring,

(a)double fold , (b) triply; (c) four- fold- symmetry of the loads

ISSN 2347-3487

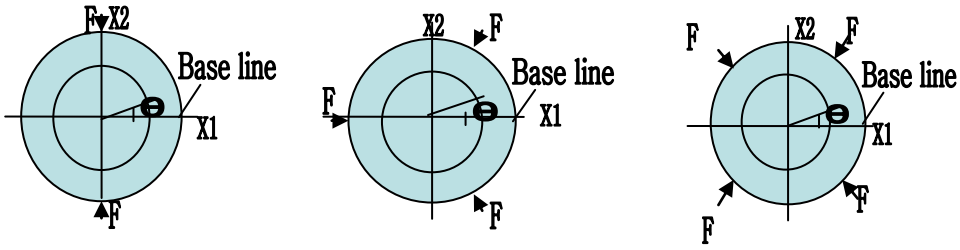

Figure 2 Symmetrical point forces F acting on outer surface of the ring
(a) Double fold (b) triply; (c) four- fold- symmetry of the loads

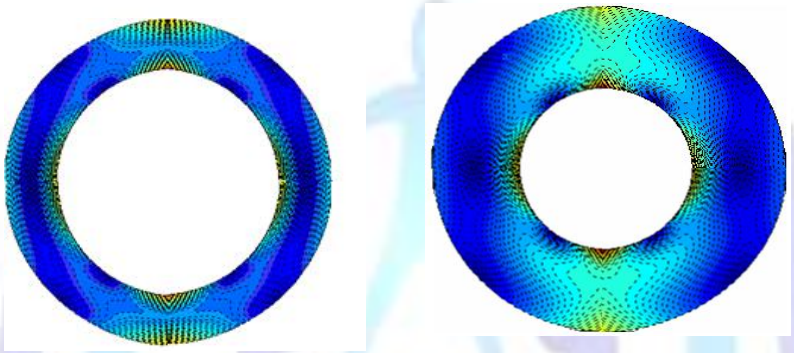

Fig.3 The graph of the equi-maximum shear stress for the double symmetrical forces , left $\alpha_i = 0.7$ (stress step 1.2 F/π r_0.) and right $\alpha_i = 0.5$ (stress step 0.4 F/π r_0.)

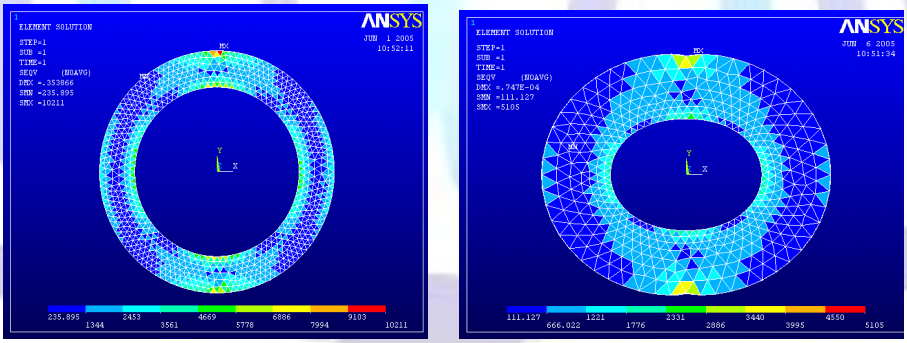

Fig4 FEM simulation results with α_i=0.7(left)and with α_i=0.5 (right)

ISSN 2347-3487

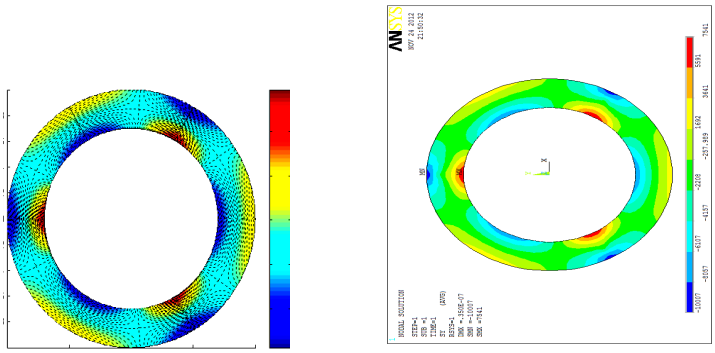

Figure 5 The graph of the circumference stress for the triple fold- symmetrical forces when $\alpha_i = 0.7$ (stress step 0.5933 F/π r_0.)

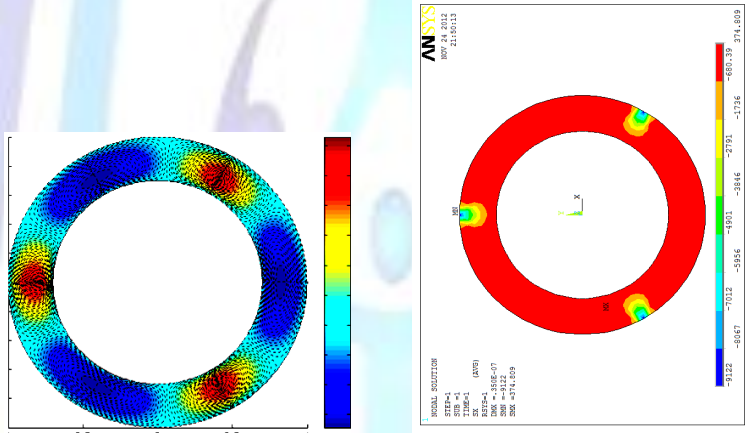

Figure 6 The graph of the radial stress for the triple fold- symmetrical forces when $\alpha_i = 0.7$ (stress step 0.0397 F/π r_0.)

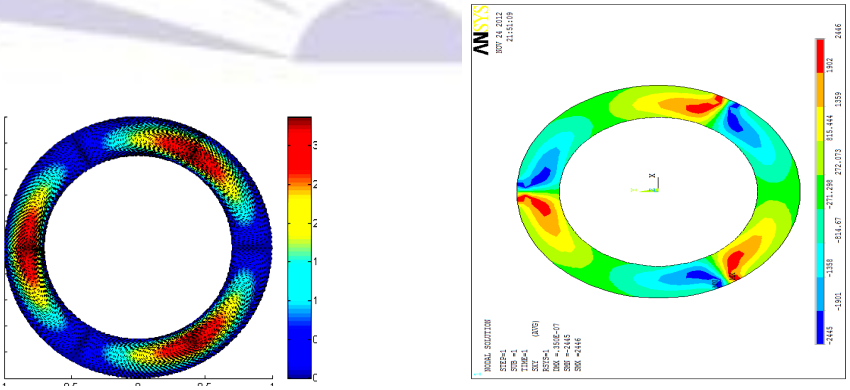

Figure 7 The graph of the shear stress for the triple fold- symmetrical forces when $\alpha_i = 0.7$ (stress step 0.0688F/π r_0.)

ISSN 2347-3487

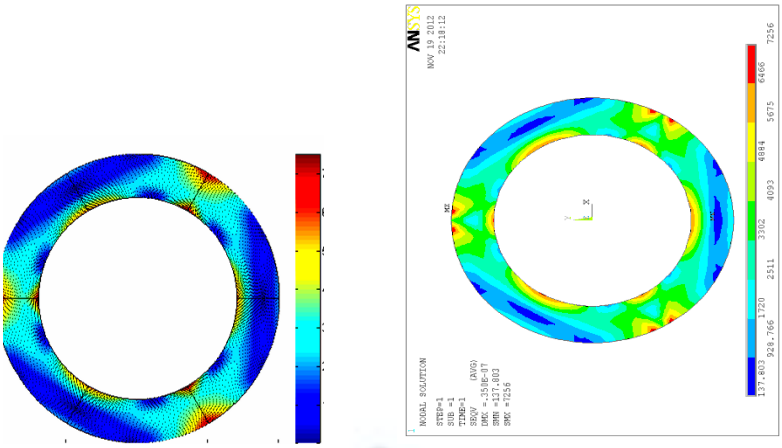

Figure 8 The graph of the equi-maximum shear stress for the triple fold- symmetrical forces when $\alpha_i = 0.7$ (stress step 0.1524 F/π r_0.)

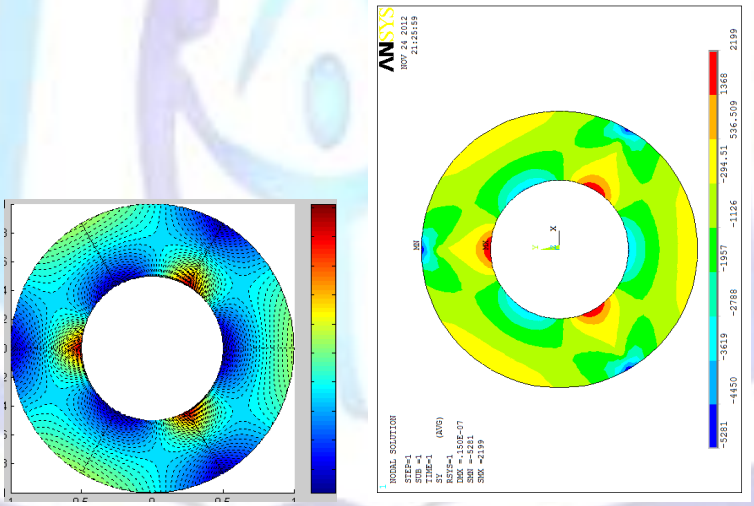

Figure 9 The graph of the circumference stress for the triple fold- symmetrical forces when $\alpha_i = 0.5$ (stress step 0.2024 F/π r_0.)

ISSN 2347-3487

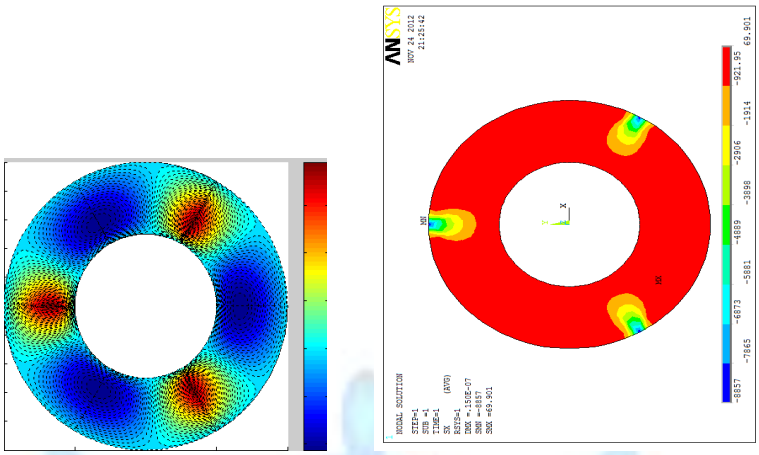

Figure 10 The graph of the radial stress for the triple fold- symmetrical forces when $\alpha_i = 0.5$ (stress step 0.0246 F/π r_0.)

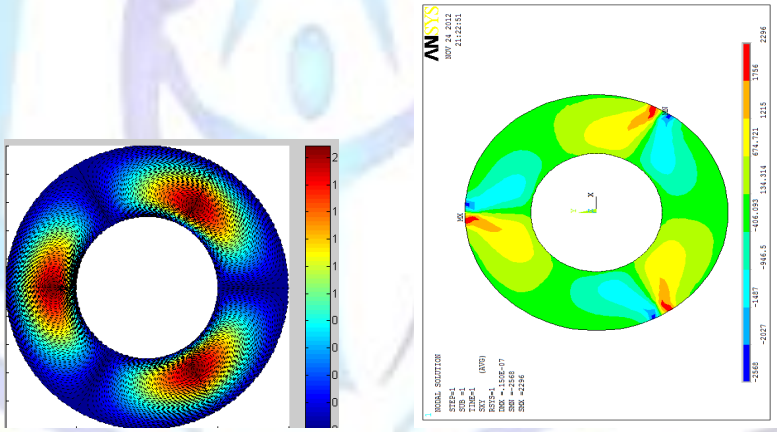

Figure 11 The graph of the shear stress for the triple fold- symmetrical forces whe n $\alpha_i = 0.5$ (stress step 0.0426 F/π r_0.)

ISSN 2347-3487

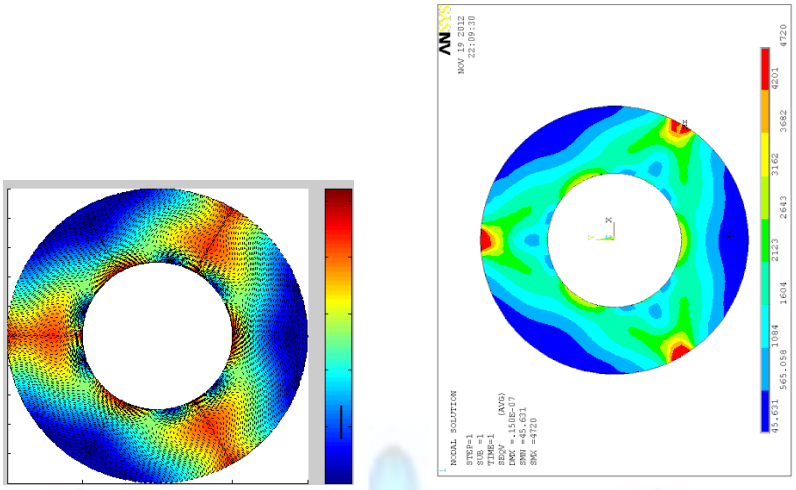

Fig.12 The graph of the equi-maximum shear stress for the triple fold- symmetrical forces when

$\alpha_i = 0.5$ **(stress step 0.0532 F/π r_0.)**

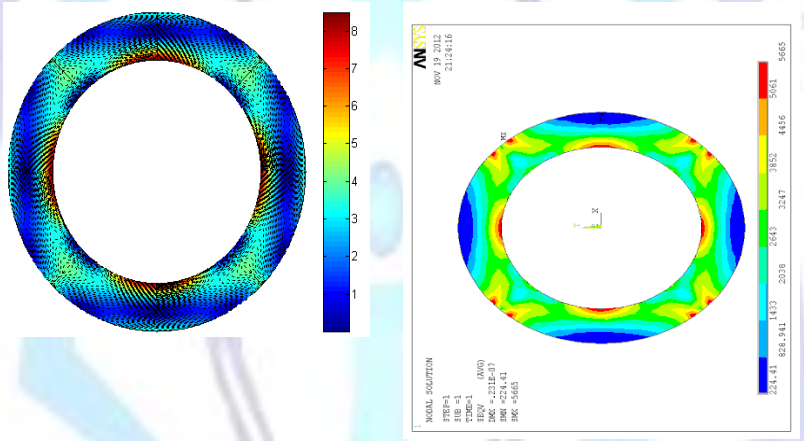

Fig.13 The graph of the equi-maximum shear stress for the four fold- symmetrical forces when

$\alpha_i = 0.7$ **(stress step 0.3464F/π r_0.)**

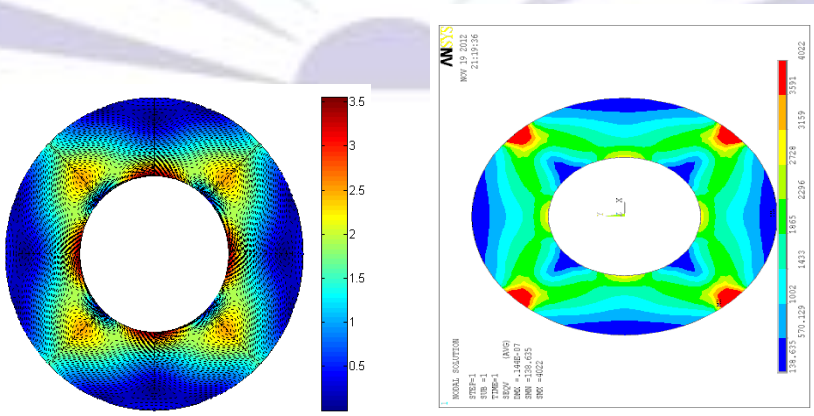

Figure 14 The graph of the equi-maximum shear stress for the four fold- symmetrical forces when

$\alpha_i = 0.5$ **(stress step 0.1446 F/π r_0**

ISSN 2347-3487

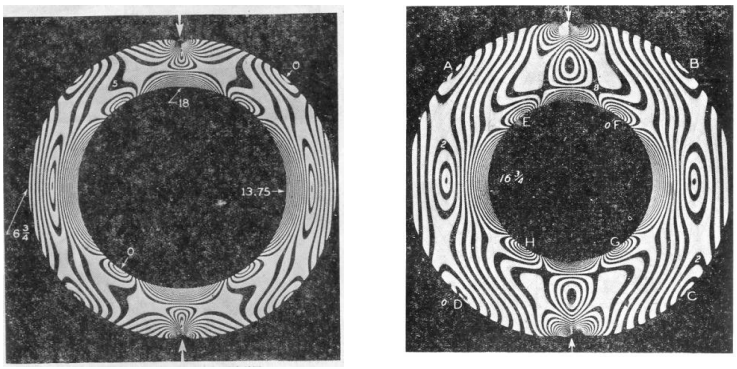

Figure 15 The experiment stripes of photo elasticity testing . left : α_i =0.7; right : α_i =0.5

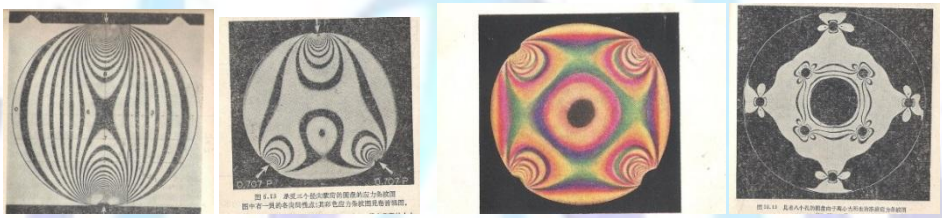

Figure 16 Photo elasticity testing results in the solid discs and 8 hole ring, pressed by different fold- symmetrical forces on them[5]

REFERENCES

[1] Timsoshenko, S., On the distribution of stress in a circular ring compressed by two forces along a diameter (J) , Phil. Mag., 1922,44 , 1014

[2] Timoshenko, S., Strength of Material, Part 1,Elementary, Third edition （M） ,1955, Van Norstrand Reinhold Company, Newyork,380.

[3] Frocht, M.M. and Hill, H.N., Stress-concentration factors around a central circular hole in a plate loaded through pin in the hole (J) . J. Appl. Mech., 1940, 7, 5

[4] Ripperger E.A. and David ,N., Critical stresses in a circular ring (J) , Proc. ASCE, February 1946

[5] Frocht, M. M., Photo Elasticity, V.1 (M) , 1946, John Wiley &Sons, 44 。

[6] Roark, R., Formulas for stress and strain (M) , 1965, McGraw-Hill, London , 333

[7] Lurje ,A.F., Theory of Elasticity (in Russian) (M) ,1970 , Nauka, Moscow

[8] Durelli ,A.J. and Lin ,Y.H.,` Stresses and displacements on the boundaries of circular rings diametrically loaded` (J) , J. Appl, Mech. , 1986,53,213-219

ISSN 2347-3487

[9] Ma, D., Elastic stress solution for a ring subjected to point-loaded compression （J）, Int. J. Pre. Ves. & Piping, 1990, 42,185-191

[10] Ma, D., Elastic stress solution for a ring subjected to point-loaded tension （J）, Int. J. Pre. Ves. & Piping, 1991, 45,199-205

[11] Batista ,M. and Usenik, Stresses in a circular ring under two forces acting along a diameter（J）, J. Strain analysis, 1996,31 (1), 75-78

[12] Timoshenko, S., Theory of Elasticity（M）, 1934, (McGraw-Hill Book Co.),104

[13] Airy, G. B., Br. Assoc. Adv. Sci. Rep. 1862

[14] Hirth, J.P. and Lothe ,J., Theory of dislocations（M） , 1968, (McGaw-Hill Book Co.), ,7

[15] Hess, M. S., The End Problem for a Laminated Elastic Strip: I. The General Solution （J）, J. Comp. Mat. 1969 3: 262-280

[16] Bradley, F. E., Development of an Airy stress function of general applicability in one, two, or three dimensions（J）, J. Appl. Phys., 1990, 67 (1),225-226

[17] Michell, J.H., 1899, Proc. London Math.Soc.,31,100

[18] Timoshenko, S. and Goodier, J.N., Theory of Elasticity（M）, 1951,(McGraw-Hill Book Co.),116

[19] Yicai Sun，Elastic Calculation of Stresses in Rings Using Airy tress Function, An International Journal：Acta Mechanic Solida Sinica，Vol 24，S. Issue，December 2011，95-106

ISSN 2347-3487

Author' biography

Wang Peng:

Wand Peng was born in Oct.,1978, graduated form Hebei University of technology,TianJin in 2011. He was promoted to associate professor in 2013. Now he is engaged in research work on mechanics, computer science,pressure sensors and measurement techniques for semiconductor.

Yi Cai Sun:

Yi Cai Sun was born in Jan., 1939, graduated from Jiaotong University, Shanghai in 1961. He was promoted to Professor in 1992. Now he is engaged in research work on mechanics, pressure sensors and measurement techniques for semiconductor.